
Volume 163, issues 1–3, November 2009 ISSN 0377-0257
ELSEVIER
Journal of Non-Newtonian Fluid Mechanics
On-line Access via:
www.elsevier.com/locate/jnnfm

J. Non-Newtonian Fluid Mech. 163 (2009) 25–34

Contents lists available at ScienceDirect

Journal of Non-Newtonian Fluid Mechanics

journal homepage: www.elsevier.com/locate/jnnfm

Perturbation solutions of Poiseuille flows of weakly compressible Newtonian liquids

Eleni G. Taliadorou [a], Marina Neophytou [b], Georgios C. Georgiou [a,*]

[a] Department of Mathematics and Statistics, University of Cyprus, P.O. Box 20537, 1678 Nicosia, Cyprus
[b] Department of Civil and Environmental Engineering, University of Cyprus, P.O. Box 20537, 1678 Nicosia, Cyprus

ARTICLE INFO

Article history:
Received 2 April 2009
Received in revised form 9 June 2009
Accepted 10 June 2009

Keywords:
Poiseuille flow
Newtonian fluid
Compressible flow
Perturbation solution

ABSTRACT

Both the planar and axisymmetric isothermal Poiseuille flows of weakly compressible Newtonian liquids with constant shear and bulk viscosities are solved up to the second-order. A linear equation of state is assumed and a perturbation analysis of the primary flow variables is performed using compressibility as the perturbation parameter. The effects of compressibility, the bulk viscosity, the aspect ratio, and the Reynolds number on the velocity and pressure fields are studied and comparisons are made with available analytical results.

1. Introduction

Laminar Poiseuille flows of weakly compressible fluids (i.e. flows corresponding to low Mach numbers) have been studied extensively in the past few decades due to their applications in many processes involving gas flows in long capillaries or at high speeds [1], such as gas flows in micro-electro-mechanical systems (MEMS) devices [2–5], liquid flows in relatively long tubes, such as waxy crude oil transport [6] and polymer extrusion [7]. Numerical solutions of weakly compressible Poiseuille flows have been presented not only for Newtonian fluids [3,8–10] but also for generalized Newtonian fluids, such as the Carreau fluid [7] and the Bingham plastic [6], and viscoelastic fluids [11].

Perturbation and other approximate solutions have also been presented in the literature for Poiseuille flows of compressible Newtonian fluids, mostly under the assumption of ideal gas flow. Prud'homme et al. [12] employed a double perturbation expansion in terms of the radius to length ratio and the relative pressure drop to approximately solve the flow of an ideal gas in a long tube under the assumptions of purely axial flow (i.e. zero radial velocity component), no radial pressure gradient, and negligible gravity. Van den Berg et al. [13] investigated the compressible laminar Newtonian flow in a capillary using a one-dimensional perturbation analysis of radially symmetric flow and two lumped perturbation parameters which could not allow the isolation of the effects of compressibility, inertia, and bulk viscosity. The same approach has been adopted by Zohar et al. [14] to obtain a solution for subsonic gas flow through microtubes and channels with wall slip. As noted by Venerus [1], in the above studies the lubrication approximation is implicitly invoked due to the assumption of zero radial pressure gradient and the corresponding solutions are expected to be sufficiently accurate for slow flow or flow in long capillaries. Venerus [1] also pointed out that in the analyses of Prud'homme et al. [12] and van den Berg et al. [13], terms of different orders of the aspect ratio have been retained in the two components of the momentum equation, which leads to the violation of the compatibility condition for the equations of motion. Venerus [1] analyzed up to the second order the axisymmetric Poiseuille flow relaxing the lubrication approximation assumption using the streamfunction/vorticity formulation with a linear equation of state (relating the density to the pressure), and employing compressibility as the single perturbation parameter. In contrast with previous analyses, he found both a non-zero radial velocity and non-zero radial pressure gradient. Much earlier, Schwartz [15] studied the plane Poiseuille flow using a fourth-order perturbation expansion in the parameter (Mach number)^2/Reynolds number. His perturbation scheme was based on the principle of slow variation, which implies that the flow properties vary slowly with distance along the channel for sufficiently small viscosity and/or mass flow rate. He also assumed that the fluid is a thermally perfect gas (i.e. the density is proportional to the pressure) and that the bulk viscosity is zero.

In the present work we derive second order perturbation solutions for both the planar and axisymmetric isothermal Poiseuille flows of weakly compressible Newtonian liquids. Following

* Corresponding author. Tel.: +357 22892612; fax: +357 22892601.
E-mail address: georgios@ucy.ac.cy (G.C. Georgiou).

0377-0257/$ – see front matter © 2009 Elsevier B.V. All rights reserved.
doi:10.1016/j.jnnfm.2009.06.003

Venerus [1], a linear equation of state is employed and the isothermal compressibility is taken as the perturbation parameter. Moreover, both the shear and bulk viscosities are assumed to be constant (independent of the pressure) and the no-slip boundary condition is assumed along the wall. However, instead of using a vorticity/streamfunction formulation, only the primary unknown fields are perturbed in the present work. In the following sections, explicit analytical solutions for pressure, density, and velocity are obtained up to the second order. These agree (up to the second order) with the solution of Schwartz [15] at the exit of the channel. The derivation of the solution of the axisymmetric flow is provided in the Appendix A. The effects of compressibility, the Reynolds number, the aspect ratio, and the bulk viscosity on the velocity and pressure fields are also discussed.

2. Governing equations

The constitutive equation of a compressible Newtonian fluid is

$$\boldsymbol{\tau} = \eta[\nabla \mathbf{u} + (\nabla \mathbf{u})^T] + \left(\kappa - \frac{2}{3}\eta\right) \nabla \cdot \mathbf{u}\,\mathbf{I}, \tag{1}$$

where $\boldsymbol{\tau}$ is the viscous stress tensor, $\mathbf{u}$ is the velocity vector, $\nabla\mathbf{u}$ is the velocity gradient tensor, $\mathbf{I}$ is the unit tensor, η denotes the viscosity, and κ is the bulk (or dilatational) viscosity. In the present work, both η and κ are assumed to be constant, i.e. independent of pressure. Note that the bulk viscosity κ, which is very often neglected, is identically zero only for monoatomic gases at low density. This becomes important in polyatomic gases, in liquids containing gas bubbles [16], and in liquids in general [1].

We consider the steady, two-dimensional, planar isothermal Poiseuille flow of a weakly compressible Newtonian fluid under zero gravity and no slip at the walls. Under these assumptions the continuity and the x- and y-components of the Navier–Stokes equation become:

$$\frac{\partial}{\partial x}(\rho u_x) + \frac{\partial}{\partial y}(\rho u_y) = 0, \tag{2}$$

$$\rho\left(u_x\frac{\partial u_x}{\partial x} + u_y\frac{\partial u_x}{\partial y}\right) = -\frac{\partial P}{\partial x} + \eta\left(\frac{\partial^2 u_x}{\partial x^2} + \frac{\partial^2 u_x}{\partial y^2}\right) + \left(\kappa + \frac{\eta}{3}\right)\left(\frac{\partial^2 u_y}{\partial x \partial y} + \frac{\partial^2 u_x}{\partial x^2}\right), \tag{3}$$

and

$$\rho\left(u_x\frac{\partial u_y}{\partial x} + u_y\frac{\partial u_y}{\partial y}\right) = -\frac{\partial P}{\partial y} + \eta\left(\frac{\partial^2 u_y}{\partial x^2} + \frac{\partial^2 u_y}{\partial y^2}\right) + \left(\kappa + \frac{\eta}{3}\right)\left(\frac{\partial^2 u_x}{\partial x \partial y} + \frac{\partial^2 u_y}{\partial y^2}\right), \tag{4}$$

where ρ is the fluid density, u_x and u_y are respectively the horizontal and transverse velocity components, and P is the pressure. The fluid density is assumed to obey a linear equation of state:

$$\rho = \rho_0[1 + \beta(P - P_0)], \tag{5}$$

where β is the isothermal compressibility,

$$\beta \equiv -\frac{1}{V_0}\left(\frac{\partial V}{\partial P}\right)_{P_0,T} \tag{6}$$

assumed to be constant, V is the specific volume, ρ_0 and V_0 are, respectively, the density and the specific volume at a reference pressure P_0, and T is the temperature. Taking as the characteristic velocity of the flow the velocity

$$U = \frac{\dot{M}}{\rho_0 H W},$$

where $\dot{M}$ is the mass flow rate, H is the channel half width, and W is the unit length in the x-direction, we define the Mach number by

$$Ma \equiv \frac{U}{\sigma}, \tag{7}$$

where

$$\sigma = \left[\gamma\left(\frac{\partial P}{\partial \rho}\right)_T\right]^{1/2} = \left(\frac{\gamma}{\beta\rho_0}\right)^{1/2} \tag{8}$$

is the speed of sound in the fluid, γ being the heat capacity ratio (or adiabatic index). In this work we consider subsonic flows so that $Ma \ll 1$.

To nondimensionalize the governing equations, we scale x by L, y by H, ρ by the reference density ρ_0, u_x by U, the transverse velocity u_y by UH/L, and the pressure by $3\eta LU/H^2$. The latter pressure scale is used so that the dimensionless pressure gradient along the domain, in the incompressible flow is equal to 1. For the sake of simplicity, in what follows we will use the same symbols (i.e. without stars) for all dimensionless variables. Using the above scalings, the dimensionless forms of the equation of state, the continuity equation and momentum equations become:

$$\rho = 1 + \varepsilon P, \tag{9}$$

$$\frac{\partial}{\partial x}(\rho u_x) + \frac{\partial}{\partial y}(\rho u_y) = 0, \tag{10}$$

$$\alpha\, Re\rho\left(u_x\frac{\partial u_x}{\partial x} + u_y\frac{\partial u_x}{\partial y}\right) = -3\frac{\partial P}{\partial x} + \alpha^2\frac{\partial^2 u_x}{\partial x^2} + \frac{\partial^2 u_x}{\partial y^2} + \alpha^2\left(\chi + \frac{1}{3}\right)\left(\frac{\partial^2 u_y}{\partial x \partial y} + \frac{\partial^2 u_x}{\partial x^2}\right), \tag{11}$$

$$\alpha^3\, Re\rho\left(u_x\frac{\partial u_y}{\partial x} + u_y\frac{\partial u_y}{\partial y}\right) = -3\frac{\partial P}{\partial y} + \alpha^4\frac{\partial^2 u_y}{\partial x^2} + \alpha^2\frac{\partial^2 u_y}{\partial y^2} + \alpha^2\left(\chi + \frac{1}{3}\right)\left(\frac{\partial^2 u_x}{\partial x \partial y} + \frac{\partial^2 u_y}{\partial y^2}\right), \tag{12}$$

where $\chi \equiv \kappa/\eta$ is the bulk-to-shear viscosity ratio, $\alpha \equiv H/L$ is the aspect ratio of the channel, and Re and ε are, respectively, the Reynolds and compressibility numbers, which are defined by

$$Re \equiv \frac{\rho_0 U H}{\eta} \tag{13}$$

and

$$\varepsilon \equiv \frac{3\eta\beta L U}{H^2}. \tag{14}$$

The Mach number takes the form

$$Ma \equiv \sqrt{\frac{\varepsilon\alpha\, Re}{3\gamma}}.$$

The system of partial differential equations (10)–(12) is supplemented by appropriate boundary conditions. Along the wall, it is assumed that no slip occurs and the transverse velocity component vanishes (impermeable wall):

$$u_x(x, 1) = u_y(x, 1) = 0, \quad 0 \le x \le 1. \tag{15}$$

Along the midplane, the usual symmetry conditions are employed:

$$\frac{\partial u_x}{\partial y}(x, 0) = u_y(x, 0) = 0, \quad 0 \le x \le 1. \tag{16}$$

At the exit plane, the dimensionless mass flow rate is set at a value of 1:

$$\int_0^1 \rho u_x \, dy = 1. \tag{17}$$

Finally, the pressure is set to zero at $x = y = 1$:

$$P(1, 1) = 0. \tag{18}$$

As in [1], no boundary conditions are specified at the inlet plane. For an interesting discussion on the inlet and outlet boundary conditions, the reader is referred to the articles of Poinsot and Lele [17] and Venerus [1].

3. Perturbation solution

Eqs. (9)–(12) constitute a nonlinear system of PDEs that cannot be solved analytically. By using perturbation methods, approximate solutions of the flow can be obtained. As already discussed, different perturbation parameters have been used in the literature. The compressibility number, ε, is chosen here as the perturbation parameter. This choice has also been made by Venerus [1] and [15]. The latter author used the parameter (Mach number)^2/Reynolds number at $x = 1$, which is equivalent to the compressibility number used here. Prud'homme et al. [12] employed a double perturbation expansion in terms of the aspect ratio and the relative pressure drop.

As already mentioned, perturbation is performed on all primary variables, ρ, u_x, u_y, and P using the compressibility number, ε, as the perturbation parameter:

$$\left.\begin{aligned} \rho &= \rho^{(0)} + \varepsilon\rho^{(1)} + \varepsilon^2\rho^{(2)} + O(\varepsilon^3) \\ u_y &= u_y^{(0)} + \varepsilon u_y^{(1)} + \varepsilon^2 u_y^{(2)} + O(\varepsilon^3) \\ u_x &= u_x^{(0)} + \varepsilon u_x^{(1)} + \varepsilon^2 u_x^{(2)} + O(\varepsilon^3) \\ P &= P^{(0)} + \varepsilon P^{(1)} + \varepsilon^2 P^{(2)} + O(\varepsilon^3) \end{aligned}\right\}. \tag{19}$$

Substituting the above expressions into the governing equations (9)–(12) and collecting terms of the same order in the perturbation parameter ε, we get a regular perturbation scheme. The solutions up to the second order are provided below. For the zero- and the first-order equations it is assumed that the transverse velocity u_y is zero throughout the domain. For the second-order equations it is assumed that $u_y = u_y(y)$ and that its second derivatives at the wall and the plane of symmetry are equal to zero.

3.1. Zero-order solution

The zero-order equations are:

$$\rho^{(0)} = 1,$$

$$\frac{\partial}{\partial x}[\rho^{(0)} u_x^{(0)}] + \frac{\partial}{\partial y}[\rho^{(0)} u_y^{(0)}] = 0,$$

$$\alpha\, Re\rho^{(0)} \left[u_x^{(0)} \frac{\partial u_x^{(0)}}{\partial x} + u_y^{(0)} \frac{\partial u_x^{(0)}}{\partial y} \right] = -3\frac{\partial P^{(0)}}{\partial x} + \frac{\partial^2 u_x^{(0)}}{\partial y^2} + \alpha^2 \frac{\partial^2 u_x^{(0)}}{\partial x^2} + \alpha^2 \left(\chi + \frac{1}{3}\right) \left[\frac{\partial^2 u_y^{(0)}}{\partial x \partial y} + \frac{\partial^2 u_x^{(0)}}{\partial x^2} \right],$$

and

$$\alpha^3\, Re\rho^{(0)} \left[u_x^{(0)} \frac{\partial u_y^{(0)}}{\partial x} + u_y^{(0)} \frac{\partial u_y^{(0)}}{\partial y} \right] = -3\frac{\partial P^{(0)}}{\partial y} + \alpha^4 \frac{\partial^2 u_y^{(0)}}{\partial x^2} + \alpha^2 \frac{\partial^2 u_y^{(0)}}{\partial y^2} + \alpha^2 \left(\chi + \frac{1}{3}\right) \left[\frac{\partial^2 u_x^{(0)}}{\partial x \partial y} + \frac{\partial^2 u_y^{(0)}}{\partial y^2} \right].$$

With the assumptions $u_y^{(0)}(x, y) = 0$ and $P^{(0)}(x = 0) = 1$, the zero-order solution is easily obtained:

$$\rho^{(0)} = 1, \tag{20}$$

$$u_y^{(0)} = 0, \tag{21}$$

$$u_x^{(0)} = \frac{3}{2}(1 - y^2), \tag{22}$$

$$P^{(0)} = 1 - x. \tag{23}$$

Obviously, the above solution is the solution of the incompressible Newtonian planar Poiseuille flow.

3.2. First-order solution

The first-order equations are:

$$\rho^{(1)} = P^{(0)}(x),$$

$$\frac{\partial}{\partial x}[\rho^{(0)} u_x^{(1)} + \rho^{(1)} u_x^{(0)}] + \frac{\partial}{\partial y}[\rho^{(0)} u_y^{(1)} + \rho^{(1)} u_y^{(0)}] = 0,$$

$$\begin{aligned} &\alpha\, Re\rho^{(1)} \left[u_x^{(0)} \frac{\partial u_x^{(0)}}{\partial x} + u_y^{(0)} \frac{\partial u_x^{(0)}}{\partial y} \right] + \alpha\, Re\rho^{(0)} \left[u_x^{(0)} \frac{\partial u_x^{(1)}}{\partial x} + u_x^{(1)} \frac{\partial u_x^{(0)}}{\partial x} + u_y^{(0)} \frac{\partial u_x^{(1)}}{\partial y} + u_y^{(1)} \frac{\partial u_x^{(0)}}{\partial y} \right] \\ &= -3\frac{\partial P^{(1)}}{\partial x} + \frac{\partial^2 u_x^{(1)}}{\partial y^2} + \alpha^2 \frac{\partial^2 u_x^{(1)}}{\partial x^2} + \alpha^2 \left(\chi + \frac{1}{3}\right) \left[\frac{\partial^2 u_y^{(1)}}{\partial x \partial y} + \frac{\partial^2 u_x^{(1)}}{\partial x^2} \right], \end{aligned}$$

and

$$\begin{aligned} &\alpha^3\, Re\rho^{(1)} \left[u_x^{(0)} \frac{\partial u_y^{(0)}}{\partial x} + u_y^{(0)} \frac{\partial u_y^{(0)}}{\partial y} \right] + \alpha^3\, Re\rho^{(0)} \left[u_x^{(0)} \frac{\partial u_y^{(1)}}{\partial x} + u_x^{(1)} \frac{\partial u_y^{(0)}}{\partial x} + u_y^{(0)} \frac{\partial u_y^{(1)}}{\partial y} + u_y^{(1)} \frac{\partial u_y^{(0)}}{\partial y} \right] \\ &= -3\frac{\partial P^{(1)}}{\partial y} + \alpha^4 \frac{\partial^2 u_y^{(1)}}{\partial x^2} + \alpha^2 \frac{\partial^2 u_y^{(1)}}{\partial y^2} + \alpha^2 \left(\chi + \frac{1}{3}\right) \left[\frac{\partial^2 u_x^{(1)}}{\partial x \partial y} + \frac{\partial^2 u_y^{(1)}}{\partial y^2} \right]. \end{aligned}$$

Obviously, $\rho^{(1)} = P^{(0)}(x) = 1 - x$. Assuming that $u_y^{(1)}(x, y) = 0$, we find from the continuity and the y-momentum equations that

$$u_x^{(1)} = -\frac{3}{2}(1-x)(1-y^2) + f(y)$$

and

$$P^{(1)} = \frac{1}{2}\alpha^2\left(\chi + \frac{1}{3}\right)(1-y^2) + g(x),$$

where $f(y)$ and $g(x)$ are unknown functions. Substituting into the x-momentum equation and separating variables we get

$$\frac{9}{4}\alpha\, Re(1-y^2)^2 - f''(y) = -3\frac{\partial P^{(1)}}{\partial x} + 3(1-x) = c,$$

where c is a constant to be determined. Integrating the resulting ODEs and applying the boundary conditions $f'(0) = f(1) = 0$ and $\int_0^1 f(y)\, dy = 0$ for $u_x^{(1)}(x, y)$ and $P^{(1)}(1, 1) = 0$ for $P(x, y)$ we find that $c = 54/35\alpha\, Re$ and the functions $g(x)$ and $f(y)$. The first-order solution reads:

$$\rho^{(1)} = 1 - x, \tag{24}$$

$$u_y^{(1)} = 0, \tag{25}$$

$$u_x^{(1)} = -\frac{3}{2}(1-x)(1-y^2) + \frac{3}{280}\alpha\, Re(1-y^2)(-5 + 28y^2 - 7y^4), \tag{26}$$

$$P^{(1)} = \frac{1}{2}\alpha^2\left(\chi + \frac{1}{3}\right)(1-y^2) - \frac{1}{2}(1-x)^2 + \frac{18}{35}\alpha\, Re(1-x). \tag{27}$$

We observe that the first-order pressure is a function of both x and y. It should also be noted that the assumption of zero, first-order transverse velocity is made implicitly in the analysis of Venerus [1] for the axisymmetric flow, since simple functional forms for the first-order vorticity and streamfunction are assumed instead.

3.3. Second-order solution

The equations governing the second-order solution are:

$$\rho^{(2)} = P^{(1)}(x, y),$$

$$\frac{\partial}{\partial x}[\rho^{(0)}u_x^{(2)} + \rho^{(1)}u_x^{(1)} + \rho^{(2)}u_x^{(0)}] + \frac{\partial}{\partial y}[\rho^{(0)}u_y^{(2)} + \rho^{(1)}u_y^{(1)} + \rho^{(2)}u_y^{(0)}] = 0,$$

$$\begin{aligned}
&\alpha\, Re\rho^{(2)}\left[u_x^{(0)}\frac{\partial u_x^{(0)}}{\partial x} + u_y^{(0)}\frac{\partial u_x^{(0)}}{\partial y}\right] \\
&+ \alpha\, Re\rho^{(1)}\left[u_x^{(0)}\frac{\partial u_x^{(1)}}{\partial x} + u_x^{(1)}\frac{\partial u_x^{(0)}}{\partial x} + u_y^{(0)}\frac{\partial u_x^{(1)}}{\partial y} + u_y^{(1)}\frac{\partial u_x^{(0)}}{\partial y}\right] \\
&+ \alpha\, Re\rho^{(0)}\left[u_x^{(0)}\frac{\partial u_x^{(2)}}{\partial x} + u_x^{(1)}\frac{\partial u_x^{(1)}}{\partial x} + u_x^{(2)}\frac{\partial u_x^{(0)}}{\partial x} + u_y^{(0)}\frac{\partial u_x^{(2)}}{\partial y}\right. \\
&\left. + u_y^{(1)}\frac{\partial u_x^{(1)}}{\partial y} + u_y^{(2)}\frac{\partial u_x^{(0)}}{\partial y}\right] \\
&= -3\frac{\partial P^{(2)}}{\partial x} + \frac{\partial^2 u_x^{(2)}}{\partial y^2} + \alpha^2\frac{\partial^2 u_x^{(2)}}{\partial x^2} \\
&+ \alpha^2\left(\chi + \frac{1}{3}\right)\left[\frac{\partial^2 u_y^{(2)}}{\partial x \partial y} + \frac{\partial^2 u_x^{(2)}}{\partial x^2}\right],
\end{aligned}$$

and

$$\begin{aligned}
&\alpha^3\, Re\rho^{(2)}\left[u_x^{(0)}\frac{\partial u_y^{(0)}}{\partial x} + u_y^{(0)}\frac{\partial u_y^{(0)}}{\partial y}\right] \\
&+ \alpha^3\, Re\rho^{(1)}\left[u_x^{(0)}\frac{\partial u_y^{(1)}}{\partial x} + u_x^{(1)}\frac{\partial u_y^{(0)}}{\partial x} + u_y^{(0)}\frac{\partial u_y^{(1)}}{\partial y} + u_y^{(1)}\frac{\partial u_y^{(0)}}{\partial y}\right] \\
&+ \alpha^3\, Re\rho^{(0)}\left[u_x^{(0)}\frac{\partial u_y^{(2)}}{\partial x} + u_x^{(1)}\frac{\partial u_y^{(1)}}{\partial x} + u_x^{(2)}\frac{\partial u_y^{(0)}}{\partial x} + u_y^{(0)}\frac{\partial u_y^{(2)}}{\partial y}\right. \\
&\left. + u_y^{(1)}\frac{\partial u_y^{(1)}}{\partial y} + u_y^{(2)}\frac{\partial u_y^{(0)}}{\partial y}\right] \\
&= -3\frac{\partial P^{(2)}}{\partial y} + \alpha^2\frac{\partial^2 u_y^{(2)}}{\partial y^2} + \alpha^4\frac{\partial^2 u_y^{(2)}}{\partial x^2} \\
&+ \alpha^2\left(\chi + \frac{1}{3}\right)\left[\frac{\partial^2 u_x^{(2)}}{\partial x \partial y} + \frac{\partial^2 u_y^{(2)}}{\partial y^2}\right].
\end{aligned}$$

For $\rho^{(2)}$ we simply have:

$$\rho^{(2)} = P^{(1)}(x, y) = \frac{1}{2}\alpha^2\left(\chi + \frac{1}{3}\right)(1-y^2) - \frac{1}{2}(1-x)^2 + \frac{18}{35}\alpha\, Re(1-x). \tag{28}$$

At this point the assumption of zero transverse velocity is relaxed, letting u_y to be a function of y, $u_y^{(2)} = u_y^{(2)}(y)$. Note again that in the analysis of Venerus [1] for the axisymmetric flow, the simplest expressions for the second-order vorticity and streamfunction are postulated instead. From the continuity and y-momentum equations we respectively get:

$$\begin{aligned}
u_x^{(2)} = &\frac{9}{4}(1-x)^2(1-y^2) - \frac{3}{4}\alpha^2\left(\chi + \frac{1}{3}\right)(1-y^2)^2 \\
&- \frac{3}{280}\alpha\, Re(1-x)(1-y^2)(67 + 28y^2 - 7y^4) \\
&+ \frac{\partial u_y^{(2)}}{\partial y}(1-x) + F(y)
\end{aligned} \tag{29}$$

and

$$\begin{aligned}
P^{(2)} = &\frac{1}{3}\alpha^2\frac{\partial u_y^{(2)}}{\partial y} - \frac{3}{2}\alpha^2\left(\chi + \frac{1}{3}\right)(1-x)(1-y^2) \\
&+ \frac{1}{280}\alpha^3 Re\left(\chi + \frac{1}{3}\right)(1-y^2)(67 + 28y^2 - 7y^4) + G(x),
\end{aligned} \tag{30}$$

where $F(y)$ and $G(x)$ are functions to be determined. Combining Eqs. (28)–(30) and the x-momentum equation leads to:

$$\begin{aligned}
&\alpha\, Re\left[-3yu_y^{(2)} - \frac{3}{2}(1-y^2)\frac{\partial u_y^{(2)}}{\partial y} - \frac{27}{4}(1-x)(1-y^2)^2\right. \\
&\left. + \frac{9}{560}\alpha\, Re(1-y^2)^2(62 + 56y^2 - 14y^4)\right] \\
&= -3G'(x) - \frac{9}{2}(1-x)^2 + \frac{\partial^3 u_y^{(2)}}{\partial y^3}(1-x) + F''(y) \\
&- \frac{3}{280}\alpha\, Re(1-x)(-78 - 420y^2 + 210y^4) \\
&+ \frac{9}{2}\alpha^2(1-y^2) + 3\alpha^2\left(\chi + \frac{1}{3}\right)(1-3y^2).
\end{aligned} \tag{31}$$

Here, it is assumed that the terms involving both $(1-x)$ and y must be equal to a (scalar) multiple of $(1-x)$. Thus we can assume that

$$\frac{27}{4}\alpha\,Re(1-y^2)^2+\frac{\partial^3 u_y^{(2)}}{\partial y^3}-\frac{3}{280}\alpha\,Re(-78-420y^2+210y^4)=\alpha\,Re\gamma, \tag{32}$$

where γ is new constant to be determined. Solving the above equation with the conditions $u_y^{(2)}(0)=u_y^{(2)}(1)=0$ and $\partial u_y^{(2)}/\partial y(1)=\partial^2 u_y^{(2)}/\partial y^2(0)=0$ yields $\gamma=216/35$ and the second-order transverse velocity:

$$u_y^{(2)}=\frac{3}{140}\alpha\,Re\,y(1-y^2)^2(5-y^2). \tag{33}$$

Separating variables in Eq. (31) gives the following ODEs for $F(y)$ and $G(x)$:

$$\alpha\,Re\left[-3yu_y^{(2)}-\frac{3}{2}(1-y^2)\frac{\partial u_y^{(2)}}{\partial y}+\frac{9}{560}\alpha\,Re(1-y^2)^2(62+56y^2-14y^4)\right]-F''(y)-\frac{9}{2}\alpha^2(1-y^2)-3\alpha^2\left(\chi+\frac{1}{3}\right)(1-3y^2)=A \tag{34}$$

and

$$-3G'(x)-\frac{9}{2}(1-x)^2+\alpha\,Re\gamma(1-x)=A, \tag{35}$$

where A is another constant to be determined. Integrating Eq. (34) and applying the conditions $F'(0)=F(1)=0$ and $\int_0^1 F(y)\,dy=0$ we find that

$$F(y)=\alpha^2\left(\chi+\frac{1}{3}\right)\left(\frac{3}{20}-\frac{9}{10}y^2+\frac{3}{4}y^4\right)+\alpha^2\left(\frac{3}{40}-\frac{9}{20}y^2+\frac{9}{24}y^4\right)-\frac{3}{431200}\alpha^2Re^2(2193-11356y^2+2310y^4+12012y^6-5775y^8+616y^{10}) \tag{36}$$

and

$$A=-\frac{18\alpha^2}{5}-\frac{6}{5}\alpha^2\left(\chi+\frac{1}{3}\right)+\frac{9132}{13475}\alpha^2\,Re^2. \tag{37}$$

Integrating now Eq. (35) and substituting A under the condition $P^{(2)}(1,1)=0$ we obtain

$$G(x)=\frac{1}{2}(1-x)^3-\frac{6}{5}\alpha^2(1-x)-\frac{36}{35}\alpha\,Re(1-x)^2+\frac{3044}{13475}\alpha^2Re^2(1-x)-\frac{2}{5}\alpha^2\left(\chi+\frac{1}{3}\right)(1-x). \tag{38}$$

Thus, the second order solution reads:

$$\rho^{(2)}=\frac{1}{2}\alpha^2\left(\chi+\frac{1}{3}\right)(1-y^2)-\frac{1}{2}(1-x)^2+\frac{18}{35}\alpha\,Re(1-x), \tag{39}$$

$$u_y^{(2)}=\frac{3}{140}\alpha\,Re\,y(1-y^2)^2(5-y^2), \tag{40}$$

$$u_x^{(2)}=(1-y^2)\left[\frac{9}{4}(1-x)^2-\frac{3}{280}\alpha\,Re(57+84y^2-21y^4)(1-x)+\frac{3}{40}\alpha^2(1-5y^2)-\frac{3}{5}\alpha^2\left(\chi+\frac{1}{3}\right)-\frac{3}{431200}\alpha^2\,Re^2(2193-9163y^2-6853y^4+5159y^6-616y^8)\right], \tag{41}$$

$$P^{(2)}=\frac{1}{2}(1-x)^3-\frac{6}{5}\alpha^2(1-x)-\frac{36}{35}\alpha\,Re(1-x)^2+\frac{3044}{13475}\alpha^2Re^2(1-x)-\frac{1}{10}\alpha^2\left(\chi+\frac{1}{3}\right)(19-15y^2)(1-x)+\frac{1}{280}\alpha^3Re(1-y^2)\times\left[2(5-28y^2+7y^4)+\left(\chi+\frac{1}{3}\right)(67+28y^2-7y^4)\right]. \tag{42}$$

Summarizing the results, the solution of the flow problem up to the second order is as follows:

$$\rho=1+\varepsilon(1-x)+\varepsilon^2\left[\frac{1}{2}\alpha^2\left(\chi+\frac{1}{3}\right)(1-y^2)-\frac{1}{2}(1-x)^2+\frac{18}{35}\alpha\,Re(1-x)\right]+O(\varepsilon^3), \tag{43}$$

$$u_y=\frac{3}{140}\varepsilon^2\alpha\,Re\,y(1-y^2)^2(5-y^2)+O(\varepsilon^3), \tag{44}$$

$$u_x=\frac{3}{2}(1-y^2)\left[1-\varepsilon(1-x)+\frac{1}{140}\varepsilon\alpha\,Re(-5+28y^2-7y^4)+\frac{3}{2}\varepsilon^2(1-x)^2-\frac{1}{140}\varepsilon^2\alpha\,Re(57+84y^2-21y^4)(1-x)+\frac{1}{20}\varepsilon^2\alpha^2(1-5y^2)-\frac{2}{5}\varepsilon^2\alpha^2\left(\chi+\frac{1}{3}\right)-\frac{1}{215600}\varepsilon^2\alpha^2\,Re^2(2193-9163y^2-6853y^4+5159y^6-616y^8)\right]+O(\varepsilon^3), \tag{45}$$

$$P=1-x+\frac{1}{2}\varepsilon\alpha^2\left(\chi+\frac{1}{3}\right)(1-y^2)-\frac{1}{2}\varepsilon(1-x)^2+\frac{18}{35}\varepsilon\alpha\,Re(1-x)+\frac{1}{2}\varepsilon^2(1-x)^3-\frac{6}{5}\varepsilon^2\alpha^2(1-x)-\frac{36}{35}\varepsilon^2\alpha\,Re(1-x)^2+\frac{3044}{13475}\varepsilon^2\alpha^2Re^2(1-x)-\frac{1}{10}\varepsilon^2\alpha^2\left(\chi+\frac{1}{3}\right)(19-15y^2)(1-x)+\frac{1}{280}\varepsilon^2\alpha^3Re(1-y^2)\times\left[2(5-28y^2+7y^4)+\left(\chi+\frac{1}{3}\right)(67+28y^2-7y^4)\right]+O(\varepsilon^3). \tag{46}$$

The perturbation solution for the axisymmetric flow has been also derived and is provided in the Appendix A. This is the same as the solution reported by Venerus [1] who used a vorticity/streamfunction formulation instead of working with the primary flow variables.

The basic features of the velocity and pressure fields given in Eqs. (43)–(46) are the following:

(a) The transverse velocity, u_y, which depends only on the y coordinate, is zero at first order in ε (by assumption). At second order in ε, u_y is always positive, varies linearly with the aspect ratio and the Reynolds number, and is independent of the bulk viscosity.
(b) The horizontal velocity, u_x, deviates from the parabolic incompressible solution at first order in ε due to fluid inertia. At second order in ε, there is a reduction of the horizontal velocity that is independent of inertia and enhanced by the bulk viscosity, which does not alter its parabolicity.
(c) The pressure is a function of both x and y. The y-dependence at first order in ε becomes stronger as α^2 is increased (i.e. in short channels). It also increases with the bulk viscosity. (It should be noted that there is y-dependence even when the bulk viscosity vanishes.) At second order in ε, the y-dependence of P is due not only to α and the bulk viscosity but also to inertia.
(d) The density is a decreasing function of both x and y. This is expected since the fluid is decompressed as it moves downstream and the density takes is lowest value at $x = y = 1$. At the exit of the channel ($x = 1$), for example,

$$\rho = 1 + \frac{1}{2}\varepsilon^2\alpha^2\left(\chi + \frac{1}{3}\right)(1 - y^2).$$

Since at the exit of the channel only very small variations of ρ can be acceptable, it must be $\varepsilon\alpha \ll 1$.

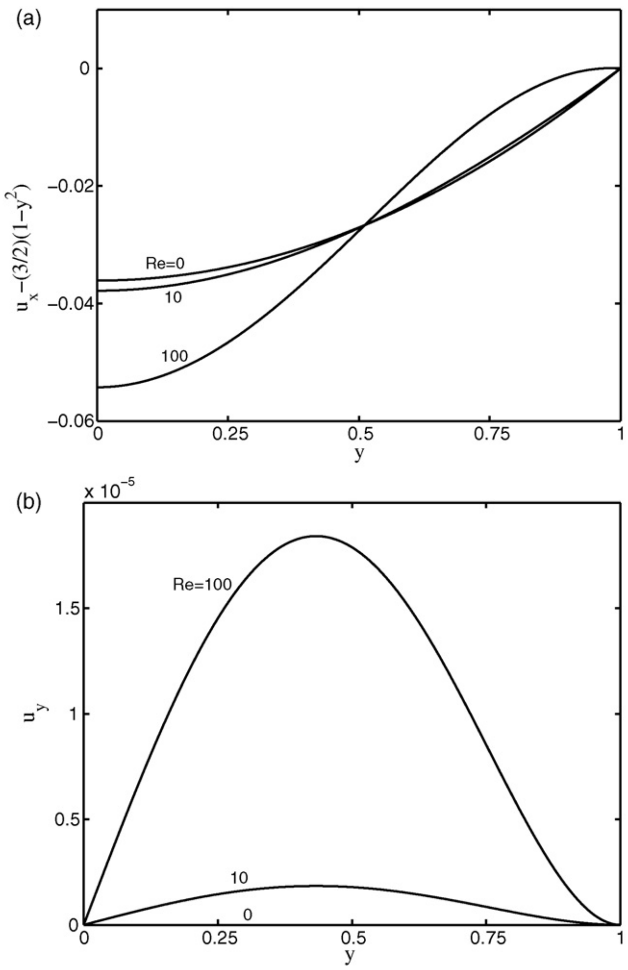

Fig. 1. Effect of the Reynolds number on the velocity components: (a) deviation of the horizontal velocity u_x from the incompressible profile; (b) transverse velocity u_y; $\varepsilon = 0.25$, $\alpha = 0.01$, $\chi = 0$, and $x = 0.9$.

In the compressible flow under study, the volumetric flow rate is an increasing function of x:

$$Q(x) = \int_0^1 u_x(x, y)\,dy = 1 - \varepsilon(1 - x) + \frac{1}{70}\varepsilon^2\left[-28\alpha^2\left(\chi + \frac{1}{3}\right) - 36\alpha\, Re(1 - x) + 105(1 - x)^2\right] + O(\varepsilon^3). \quad (47)$$

In the special case $\alpha \ll 1$, one gets $Q(0) = 1 - \varepsilon + 3\varepsilon^2/2$ which is a parabola with a minimum at $\varepsilon^* = 1/3$. Since increasing ε leads to more compression, i.e. to a lower value at $Q(0)$, the perturbation solution is valid for $\varepsilon < 1/3$. The same conclusion is reached for the axisymmetric flow (see Appendix A) for which Venerus [1] reported that the compressibility parameter is limited to values $\varepsilon \leq 0.25$.

The present results agree up to the second order with the third-order results of Schwartz [15] at $x = 1$ when $x = 1$, $\chi = 0$ and $\alpha = 3$. It is interesting to note that employing the lubrication approximation would have led to the following simplified solution [8]

$$\left.\begin{aligned} &\rho = 1 + \varepsilon P \\ &u_y = 0 \\ &u_x = \frac{3}{2}\frac{(1 - y^2)}{\sqrt{1 + 2\varepsilon(1 - x)}} \\ &P = \frac{-1 + \sqrt{1 + 2\varepsilon(1 - x)}}{\varepsilon} \end{aligned}\right\}. \quad (48)$$

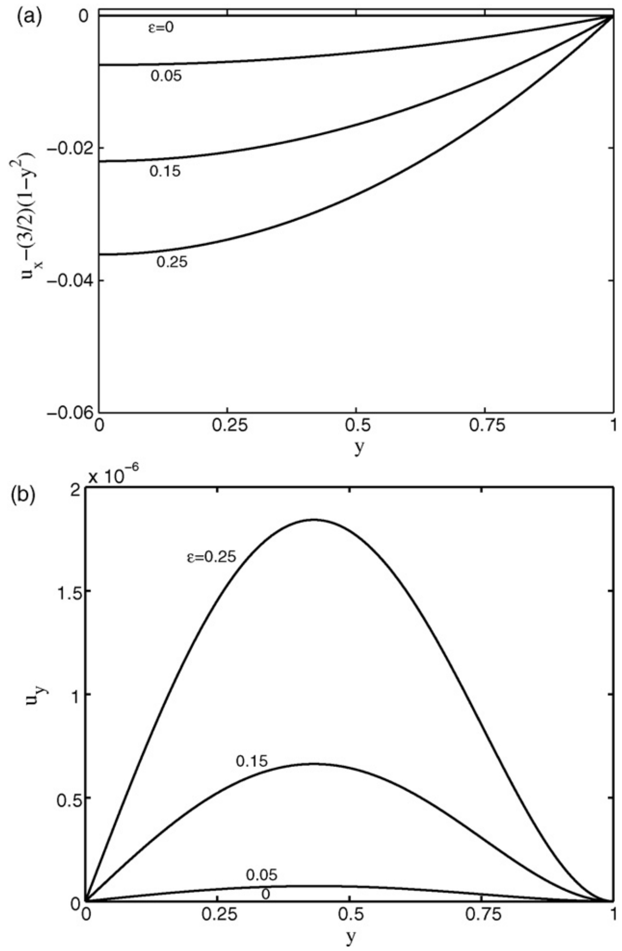

Fig. 2. Effect of compressibility on the velocity components: (a) deviation of the horizontal velocity u_x from the incompressible profile; (b) transverse velocity u_y; $Re = 10$, $\alpha = 0.01$, $\chi = 0$, and $x = 0.9$.

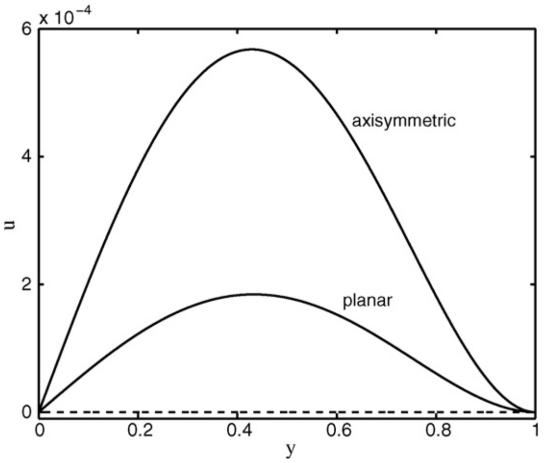

Fig. 3. Transverse velocity profiles for $\varepsilon = 0.25$, $\alpha = 0.1$ and $\alpha\,Re = 1$.

Expanding the expressions of u_x and P as power series to second order in ε leads to the approximate solution

$$\left.\begin{aligned} &\rho = 1 + \varepsilon(1-x) - \frac{1}{2}\varepsilon^2(1-x)^2 + O(\varepsilon^3) \\ &u_y = 0 \\ &u_x = \frac{3}{2}(1-y^2)\left[1 - \varepsilon(1-x) + \frac{3}{2}\varepsilon^2(1-x)^2\right] + O(\varepsilon^3) \\ &P = 1 - x - \frac{1}{2}\varepsilon(1-x)^2 + \frac{1}{2}\varepsilon^2(1-x)^3 + O(\varepsilon^3) \end{aligned}\right\}, \tag{49}$$

which involves only the compressibility parameter ε and agrees with the perturbation solution for $\alpha \ll 1$ and $Re \ll 1$.

The streamfunction, $\psi(x, y)$, defined by

$$\frac{\partial\psi}{\partial x} \equiv \rho u_y \quad \text{and} \quad \frac{\partial\psi}{\partial y} \equiv -\rho u_x \tag{50}$$

is found to be

$$\begin{aligned} \psi(x,y) = {} & \frac{1}{2}y\left(3-y^2\right) - \frac{3}{280}\varepsilon\alpha\,Re\,y(1-y^2)^2(5-y^2) \\ & + \varepsilon^2\left[\frac{3}{40}\alpha^2 y(1-y^2)^2 + \frac{3}{20}\alpha^2\left(\chi + \frac{1}{3}\right)y(1-y^2)^2\right. \\ & + \frac{3}{140}\alpha\,Re y(1-y^2)^2(5-y^2)(1-x) \\ & + \frac{9}{431200}\alpha^2\,Re^2 y(1-y^2)^2(-6579 - 1802y^2 \\ & \left. + 1589y^4 - 168y^6)\right] + O(\varepsilon^3). \end{aligned} \tag{51}$$

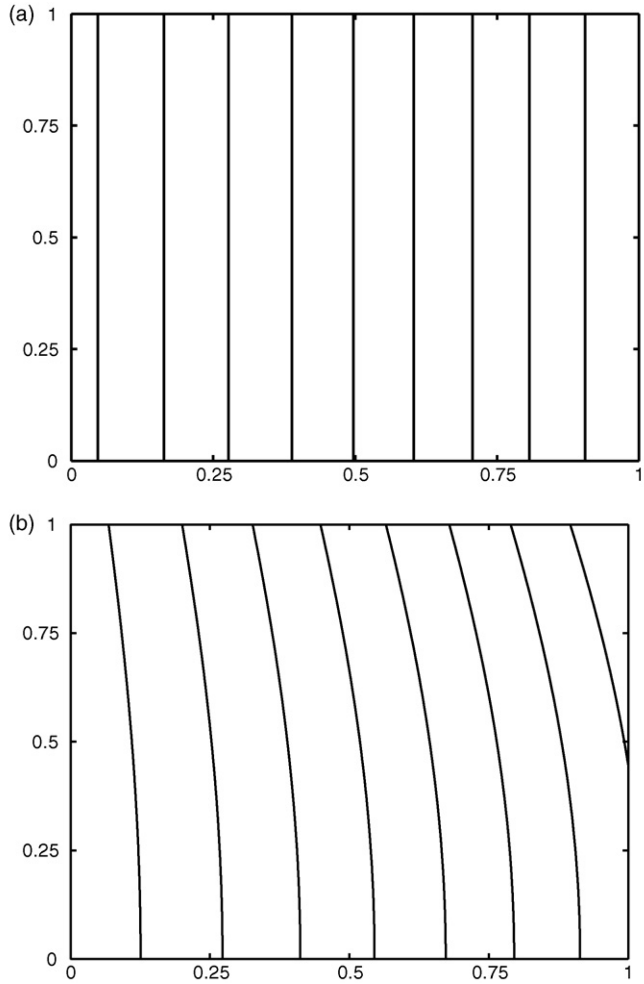

Fig. 4. Pressure field contours for plane Poiseuille flow (0.1, 0.2, ..., 0.9) with $\varepsilon = 0.25$ and $\alpha = 0.1$: (a) $\alpha\,Re = 1$, $\alpha^2(\chi + 1/3) = 0$; (b) $\alpha\,Re = 0$, $\alpha^2(\chi + 1/3) = 1$.

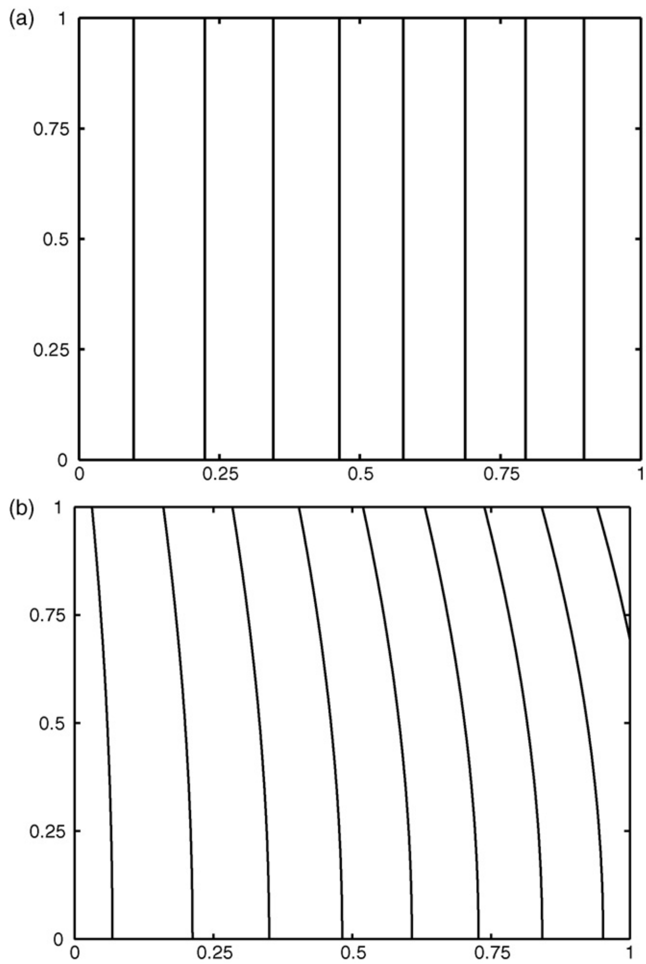

Fig. 5. Pressure field contours for plane Poiseuille flow (0.1, 0.2, ..., 0.9) with $\varepsilon = 0.25$ and $\alpha = 0.1$: (a) $\alpha\,Re = 0$, $\alpha^2(\chi + 1/3) = 0$; (b) $\alpha\,Re = 1$, $\alpha^2(\chi + 1/3) = 1$.

4. Results and discussion

The effects of all parameters involved in the solution, i.e. the compressibility number, ε, the aspect ratio, α, the Reynolds number, Re and the bulk viscosity, χ, have been studied. Mostly results for the planar compressible Poiseuille flow will be presented in this section, since the perturbation solution for the axisymmetric flow (Appendix A) is that obtained by Venerus [1].

The effects of the Reynolds number and compressibility on the two velocity components are illustrated in Figs. 1 and 2, respectively. The deviation of the horizontal velocity profile from the incompressible solution relatively close to the exit at $x = 0.9$ is shown in Fig. 1 a for different Reynolds numbers ($Re = 0$, 10, 100), $\alpha = 0.01$, and for the relatively high compressibility number $\varepsilon = 0.25$. While for low Reynolds numbers it is parabolic, the deviation from the incompressible solution becomes sigmoidal at higher Reynolds numbers. The effect of the Reynolds number on the transverse velocity, u_y, is illustrated in Fig. 1 b. It is clear from Eq. (44), that u_y is always positive, does not depend on the x coordinate and the bulk viscosity χ, and increases linearly with the Reynolds number. Fig. 2 a shows the deviation of the horizontal velocity from the incompressible flow near the exit ($x = 0.9$) for different values of ε, $Re = 10$ and $\alpha = 0.01$. It can be observed that the profile of u_x flattens as compressibility is increased. The effect of ε on the transverse velocity is shown in Fig. 2 b. As expected, u_y increases quadratically with the compressibility number. Fig. 3 shows the transverse velocity profile in both the axisymmetric and planar cases for $\varepsilon = 0.25$, $\alpha = 0.1$, $\alpha\,Re = 1$ and $\alpha^2(\chi + 1/3) = 0$. The axisymmetric result is of course identical to that of Venerus [1]. A more flattened profile is obtained in the planar case.

In Fig. 4, we show the pressure contours obtained with $\varepsilon = 0.25$ and $\alpha = 0.1$ for the two cases considered by Venerus [1]: (a) $\alpha\,Re = 1$ and $\alpha^2(\chi + 1/3) = 0$; (b) $\alpha\,Re = 0$ and $\alpha^2(\chi + 1/3) = 1$. These are similar to their axisymmetric counterparts [1]. When the channel is relatively short ($\alpha\,Re = 1$, Fig. 4a) the flow is essentially incompressible and the pressure contours are practically vertical and equidistant. For longer channels ($\alpha\,Re = 0$), however, the pressure contours are slightly parabolic as illustrated in Fig. 4 b. Moreover the distance between the contours increases upstream, due to compressibility. As pointed out by Venerus [1] this effect is due to the bulk viscosity. Note that Venerus [1] does not specify the value of α which is taken here to be equal to 0.1. In Fig. 5 we provide the pressure contours for the two complementary cases: (a) $\alpha\,Re = 0$ and $\alpha^2(\chi + 1/3) = 0$; (b) $\alpha\,Re = 1$ and $\alpha^2(\chi + 1/3) = 1$. Comparing Figs. 4 and 5, we deduce that the parameter $\alpha^2(\chi + 1/3)$ has a stronger effect on the pressure contours than $\alpha\,Re$. The velocity contours for all cases considered in Figs. 4 and 5, are given in Figs. 6 and 7, respectively.

Fig. 8 shows the horizontal velocity field deviation from the incompressible solution at various distances from the inlet plane, as given by Eq. (45) with $\varepsilon = 0.25$ and $\alpha = 0.1$ for two cases: (a) $\alpha\,Re = 1, \alpha^2(\chi + 1/3) = 0$ and (b) $\alpha\,Re = 0, \alpha^2(\chi + 1/3) = 1$. In Fig. 8 a, where the channel is relatively short the velocity profile flattens as the fluid moves downstream. For longer channels (Fig. 8b) the effect of the bulk viscosity is small and the horizontal velocity pro-

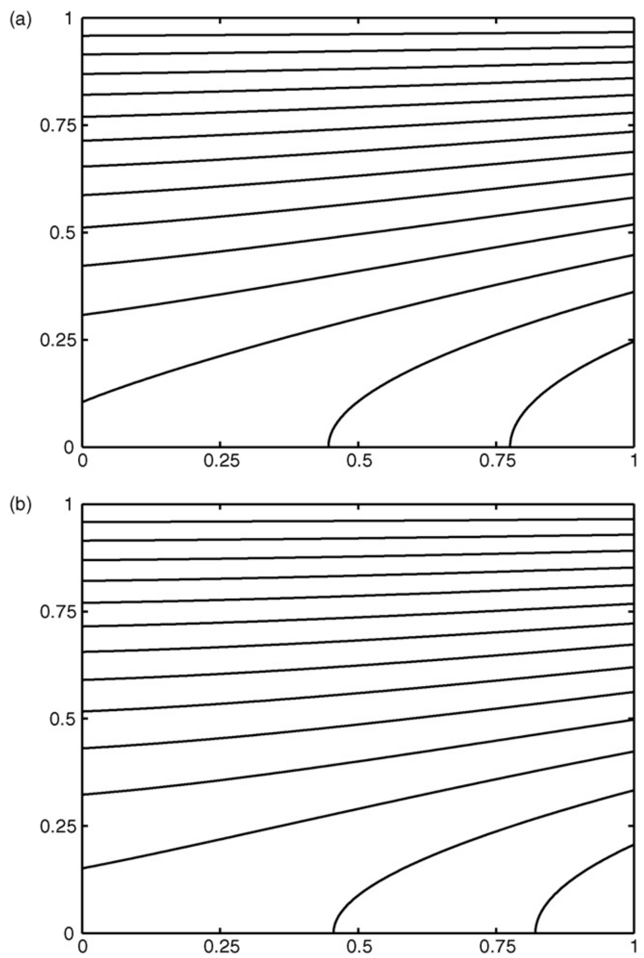

Fig. 6. Velocity field contours for plane Poiseuille flow (0.1, 0.2, ..., 1.4) with $\varepsilon = 0.25$ and $\alpha = 0.1$: (a) $\alpha\,Re = 1, \alpha^2(\chi + 1/3) = 0$; (b) $\alpha\,Re = 0, \alpha^2(\chi + 1/3) = 1$.

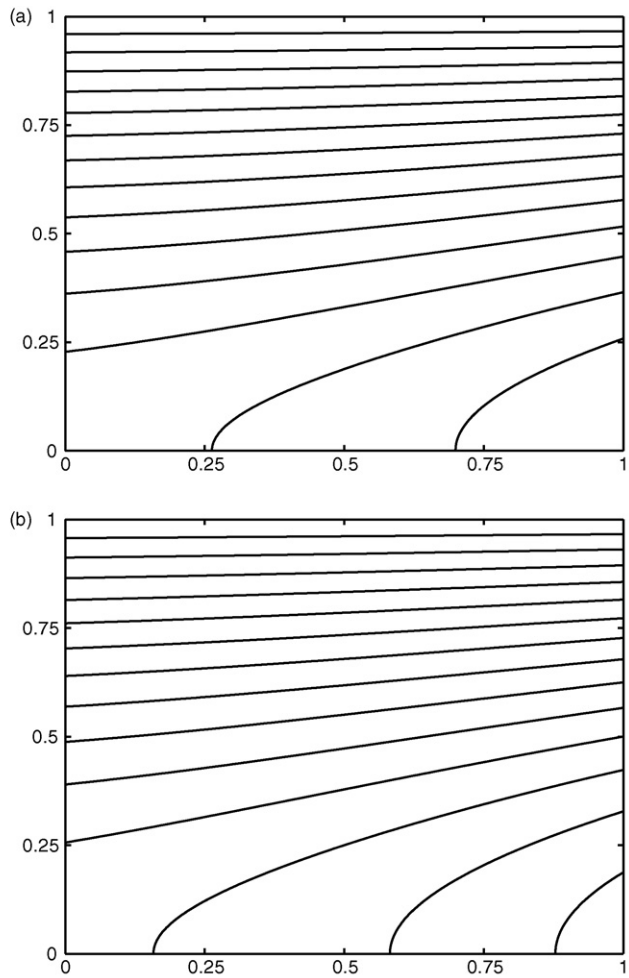

Fig. 7. Velocity field contours for plane Poiseuille flow (0.1, 0.2, ..., 1.4) with $\varepsilon = 0.25$ and $\alpha = 0.1$: (a) $\alpha\,Re = 0, \alpha^2(\chi + 1/3) = 0$; (b) $\alpha\,Re = 1, \alpha^2(\chi + 1/3) = 1$.

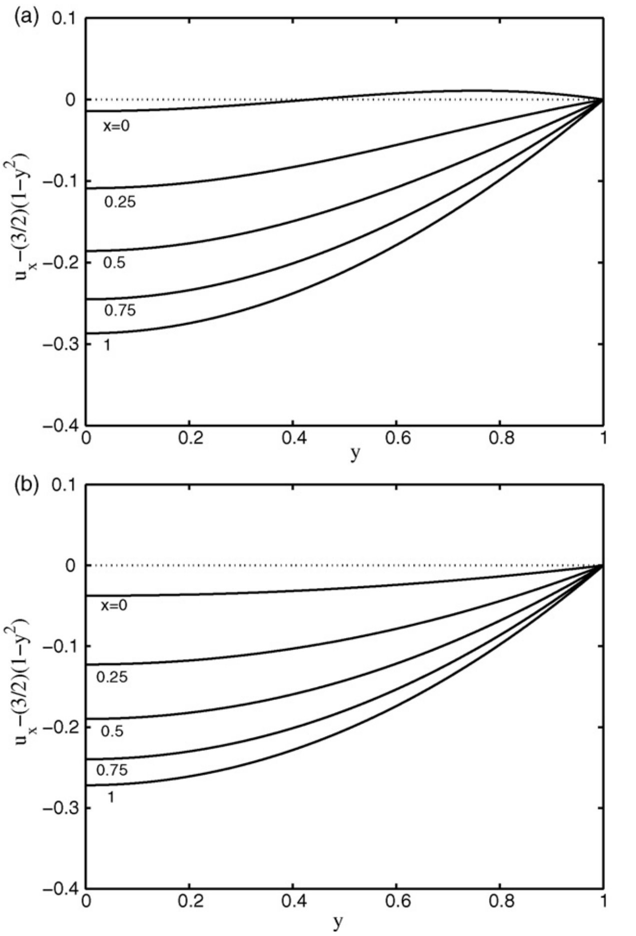

Fig. 8. Horizontal velocity field deviation from incompressible flow at various distances from the inlet plane for $\varepsilon = 0.25$ and $\alpha = 0.1$: (a) $\alpha\,Re = 1$, $\alpha^2(\chi + 1/3) = 0$; (b) $\alpha\,Re = 0$, $\alpha^2(\chi + 1/3) = 1$.

file remains parabolic. These results which are similar to those of Venerus [1] for the axisymmetric case, are also consistent with the numerical results of Guo and Wu [3,10].

Finally, Fig. 9 shows the two transverse velocity profiles obtained with (a) $Re = 100$, $\varepsilon = 0.006$ and (b) $Re = 0.01$, $\varepsilon = 0.2$ when $\alpha = 3$. The latter value of α was chosen in order to make comparisons with the results reported by Schwartz [15] at the exit $x = 1$. The present results agree with those of Schwartz [15] up to the second order.

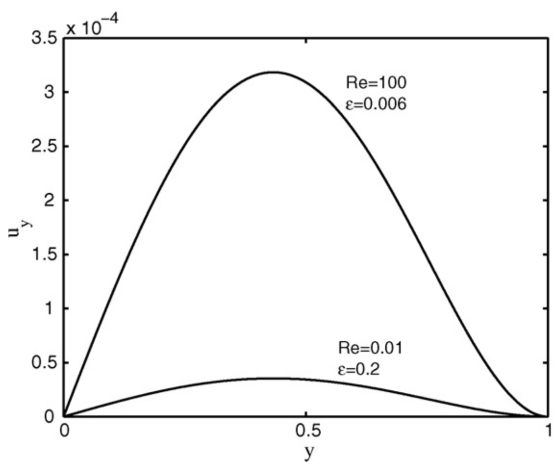

Fig. 9. Transverse velocity profiles of plane Poiseuille flow with $\alpha = 3$ and the Reynolds and compressibility numbers used by Schwartz [15].

According to Eq. (44), u_y is always positive which is not the case with the third-order solution of Schwartz [15]; this is valid only at the exit and yields negative values of u_y for small Reynolds numbers ($Re = 0.001$).

5. Conclusions

A perturbation analysis with compressibility serving as the perturbation parameter to the primary flow variables has been performed in order to solve up to second order the Navier–Stokes equations for both the planar and the axisymmetric Poiseuille flows of weakly compressible viscous fluids. For that purpose, a linear equation of state has been employed and both the shear and bulk viscosities have been taken as constants. The results for the axisymmetric flow are the same as those of Venerus [1] who employed a streamfunction/vorticity formulation. The results for the planar flow, which are similar to their axisymmetric counterparts, compare well with available results in the literature for some special cases, such as with the solution of Schwartz [15] at the exit of the channel (up to the second order). The effects of the compressibility, the Reynolds number, the aspect ratio, and the bulk viscosity on the velocity and pressure fields have been studied.

Acknowledgments

The contributions of Mrs. Lina Joseph (Oxford University) and Mrs. Savina Joseph (Imperial College London) who verified most of the derivations are gratefully acknowledged.

Appendix A. Compressible axisymmetric Poiseuille flow

The two-dimensional perturbation solution of the compressible axisymmetric Poiseuille flow is derived in this Appendix A. To nondimensionalize the equations, we scale z by L, r by R, the density by the reference density ρ_0, the axial velocity u_z by $U = \dot{M}/\rho_0\pi R^2$, the radial velocity u_r by UR/L, and the pressure by $8\eta LU/R^2$. The dimensionless forms of the governing equations are:

$$\rho = 1 + \varepsilon P, \tag{52}$$

$$\frac{1}{r}\frac{\partial}{\partial r}(r\rho u_r) + \frac{\partial}{\partial z}(\rho u_z) = 0, \tag{53}$$

$$\begin{aligned}\alpha\,Re\rho\left(u_r\frac{\partial u_z}{\partial r} + u_z\frac{\partial u_z}{\partial z}\right) &= -8\frac{\partial P}{\partial z} + \frac{1}{r}\frac{\partial}{\partial r}\left(r\frac{\partial u_z}{\partial r}\right) + \alpha^2\frac{\partial^2 u_z}{\partial z^2}\\ &\quad + \alpha^2\left(\chi + \frac{1}{3}\right)\left[\frac{\partial}{\partial z}\left(\frac{1}{r}\frac{\partial}{\partial r}(ru_r)\right) + \frac{\partial^2 u_z}{\partial z^2}\right],\end{aligned} \tag{54}$$

$$\begin{aligned}\alpha^3\,Re\rho\left(u_r\frac{\partial u_r}{\partial r} + u_z\frac{\partial u_r}{\partial z}\right) &= -8\frac{\partial P}{\partial r} + \alpha^2\frac{\partial}{\partial r}\left(\frac{1}{r}\frac{\partial}{\partial r}(ru_r)\right)\\ &\quad + \alpha^4\frac{\partial^2 u_r}{\partial z^2} + \alpha^2\left(\chi + \frac{1}{3}\right)\left[\frac{\partial}{\partial r}\left(\frac{1}{r}\frac{\partial}{\partial r}(ru_r)\right) + \frac{\partial^2 u_z}{\partial r\partial z}\right],\end{aligned} \tag{55}$$

where $\chi \equiv \dfrac{\kappa}{\eta}$, $\alpha \equiv \dfrac{R}{L}$, $Re \equiv \dfrac{\rho_0 UR}{\eta}$, and $\varepsilon \equiv \dfrac{8\eta\beta LU}{R^2}$.

The boundary conditions are similar to those used for the planar problem.

Following similar steps and making analogous assumptions as for the planar flow, we derive the following perturbation solution:

$$\rho = 1+\varepsilon(1-z) + \varepsilon^2\left[-\frac{1}{2}(1-z)^2+\frac{1}{4}\alpha\,Re(1-z)+\frac{1}{4}\alpha^2\left(\chi+\frac{1}{3}\right)(1-r^2)\right] + O(\varepsilon^3), \quad (56)$$

$$u_r = \frac{1}{36}\varepsilon^2\alpha\,Rer(1-r^2)^2(4-r^2)+O(\varepsilon^3), \quad (57)$$

$$\begin{aligned} u_z = {} & 2(1-r^2)\left[1-\varepsilon(1-z)-\frac{1}{36}\varepsilon\alpha\,Re(2-7r^2+2r^4)\right.\\ & +\frac{3}{2}\varepsilon^2(1-z)^2-\frac{1}{12}\varepsilon^2\alpha\,Re(1+7r^2-2r^4)(1-z)\\ & +\frac{1}{16}\varepsilon^2\alpha^2(1-3r^2)-\frac{1}{6}\varepsilon^2\alpha^2\left(\chi+\frac{1}{3}\right)\\ & \left.+\frac{1}{43200}\varepsilon^2\alpha^2\,Re^2(43-957r^2+2343r^4-1257r^6+168r^8)\right]\\ & +O(\varepsilon^3), \end{aligned} \quad (58)$$

$$\begin{aligned} P = {} & (1-z)-\frac{1}{2}\varepsilon(1-z)^2+\frac{1}{4}\varepsilon\alpha\,Re(1-z)+\frac{1}{4}\varepsilon\alpha^2\left(\chi+\frac{1}{3}\right)(1-r^2)\\ & +\frac{1}{2}\varepsilon^2(1-z)^3-\frac{1}{12}\varepsilon^2\alpha^2\left(\chi+\frac{1}{3}\right)(11-9r^2)(1-z)\\ & -\frac{1}{2}\varepsilon^2\alpha\,Re(1-z)^2-\frac{1}{2}\varepsilon^2\alpha^2(1-z)+\frac{1}{27}\varepsilon^2\alpha^2Re^2(1-z)\\ & +\frac{1}{144}\varepsilon^2\alpha^3\,Re(1-r^2)\\ & \times\left[(4-14r^2+4r^4)+\left(\chi+\frac{1}{3}\right)(7+7r^2-2r^4)\right]+O(\varepsilon^3). \end{aligned} \quad (59)$$

The above solution is the same as that found by Venerus [1](with the exception of a typo in his pressure expression).

References

[1] D.C. Venerus, Laminar capillary flow of compressible viscous fluids, J. Fluid Mech. 555 (2006) 59–80.
[2] E.B. Arkilic, M.A. Schmidt, K.S. Breuer, Gaseous slip flow in long microchannels, J. MEMS 6 (1995) 167–178.
[3] Z.Y. Guo, X.B. Wu, Compressibility effect on the gas flow and heat transfer in a microtube, Int. J. Heat Mass Trans. 40 (1997) 3251–3254.
[4] S. Ansumal, I.V. Karlin, Consistent lattice Boltzmann method, Phys. Rev. Lett. 95 (2005) 260605.
[5] C. Cai, Q. Sun, I.D. Boyd, Gas flows in microchannels and microtubes, J. Fluid Mech. 589 (2007) 305–314.
[6] G. Vinay, A. Wachs, I. Frigaard, Numerical simulation of weakly compressible Bingham flows: the restart of pipeline flows of waxy crude oils, J. Non-Newtonian Fluid Mech. 136 (2006) 93–105.
[7] G. Georgiou, The time-dependent, compressible Poiseuille and extrudate-swell flows of a Carreau fluid with slip at the wall, J. Non-Newtonian Fluid Mech. 109 (2003) 93–114.
[8] G.C. Georgiou, M.J. Crochet, Time-dependent compressible extrudate-swell problem with slip at the wall, J. Rheol. 38 (1994) 1745–1755.
[9] G.C. Georgiou, M.J. Crochet, Compressible viscous flow in slits with slip at the wall, J. Rheol. 38 (1994) 639–654.
[10] Z.Y. Guo, X.B. Wu, Further study on compressibility effects on the gas flow and heat transfer in a microtube, Microscale Thermophys. Eng. 2 (1998) 111–120.
[11] F. Belblidia, I.J. Keshtiban, M.F. Webster, Stabilised computations for viscoelastic flows under compressible considerations, J. Non-Newtonian Fluid Mech. 134 (2006) 56–76.
[12] R.K. Prud'homme, T.W. Chapman, J.R. Bowen, Laminar compressible flow in a tube, Appl. Sci. Res. 43 (1986) 67–74.
[13] H.R. van den Berg, C.A. ten Seldam, P.S. van der Gulik, Compressible laminar flow in a capillary, J. Fluid Mech. 246 (1993) 1–20.
[14] Y. Zohar, S.Y.K. Lee, W.Y. Lee, L. Jiang, P. Tong, Subsonic gas flow in a straight and uniform microchannel, J. Fluid Mech. 472 (2002) 125–151.
[15] L.W. Schwartz, A perturbation solution for compressible viscous channel flows, J. Eng. Math. 21 (1987) 69–86.
[16] R.B. Bird, W.E. Stewart, E.N. Lightfoot, Transport Phenomena, John Wiley, New York, 2002.
[17] T. Poinsot, S. Lele, Boundary conditions for direct simulations of compressible viscous flows, J. Comp. Phys. 101 (1992) 104–129.